Boson peak and hybridization of acoustic modes with vibrations of nanometric heterogeneities in glasses

E. Duval,[1] A. Mermet,[1] and L. Saviot[2]
[1]*Laboratoire de Physicochimie des Matériaux Luminescents, Université Lyon 1, UMR-CNRS 5620, 43 boulevard du 11 Novembre, 69622 Villeurbanne Cedex, France*
[2]*Laboratoire de Recherche sur la Réactivité des Solides, Université de Bourgogne and CNRS, Boîte Postale 47870, 21078 Dijon Cedex, France*
(Received 3 March 2006; revised manuscript received 18 July 2006; published 2 January 2007)

The low-frequency dynamics in glasses is compared with that in icosahedral quasicrystals. For both arrangements of matter, the existence of nanometric heterogeneities, implying the existence of a nanometric inhomogeneous elastic network, is expected to play a crucial role. Thanks to this comparison, mostly based on inelastic x-ray (neutron) scattering data, it is proposed that the excess of vibrational density of states observed in both materials is due to the hybridization of longitudinal and transverse acoustic modes with modes localized around the heterogeneities.

DOI: 10.1103/PhysRevB.75.024201 PACS number(s): 61.43.Fs, 71.23.Ft, 63.50.+x, 81.05.Kf

I. INTRODUCTION

The vibrational density of states excess (VDOS-EX) in comparison with the Debye regime is universally observed in glasses. It corresponds to the excess of low-temperature heat capacity or of low-frequency light Raman scattering, and is at the origin of the famous *boson peak* (conventionally defined as the VDOS divided by the frequency squared). The boson peak has been the object of many debates over more than twenty years. Depending on the composition of the glass, the harmonic vibrational modes in the VDOS-EX have frequencies distributed in a more or less broad range, i.e., in the 0.3–2 THz spectral range. The corresponding wavelengths are nanometric so that the characteristics of the vibrational modes in excess are determined by the elasticity of the glass at the nanometric scale. It has been suggested that the elasticity or the cohesion of glasses at the nanometer scale is inhomogeneous in such a way that more cohesive domains are separated by softer interdomain zones.[1,2] Within this scheme of interpretation, neither the exact shapes of the domains nor their exact nature (although most likely disordered) are expected to be known and by no means should the assumed nanostructure be mistaken for an assembly of independent clusters. The mere existence of a nanometric elastic relief suffices to generate a VDOS-EX. According to this picture, the contrast of cohesion between cohesive domains and soft zones decreases with the fragility as defined by Angell.[3] The frequency of the boson peak is approximately equal to the ratio of the sound velocity to the domain size.

In most cases it is illusory to track the heterogeneous nanostructure by techniques like small angle x-ray (neutron) scattering or microscopy because a fluctuation of elasticity can correspond to a negligible density fluctuation. A very weak variation of atomic distance can induce a relatively strong variation of cohesion. A strong support to the hypothesis of a heterogeneous nanoscaled elasticity can be found in the so-called dynamical particle mobility heterogenities observed in supercooled liquids (for a review, see Ref. 4). It is likely that the glass transition preserves a memory of these dynamical heterogenities, so that cohesion heterogeneities in glasses originate from the mobility heterogeneities in the supercooled state.

Very recently, numerical simulation works in Lennard-Jones glasses pointed out the existence of vibrational heterogeneities:[5] "hard" zones within which strongly correlated atoms have a small displacement due to harmonic vibrations, are distinguished from "soft" zones where correlated atoms have a large displacement. In other very recent simulation works,[6,7] the size of elastic heterogeneities was determined by the crossover from affine to nonaffine elasticity, and it was found that the frequency of the VDOS-EX maximum is approximately equal to the ratio of the sound velocity to the size of the elastic heterogeneity, as it was suggested earlier from experiment.[1,2]

Over the past decade, inelastic x-ray scattering (IXS) has emerged as a unique technique to probe the dispersion curves (frequency ν versus momentum Q) of phonons in glasses, throughout the THz spectral range, i.e., in the domain of nanometric wavelengths. It is generally observed that for longitudinal acoustic modes the dispersion is almost linear at least up to the frequency of the VDOS-EX maximum (ν_{max}) and sometimes beyond.[8,9] Note that ν_{max} (or $E_{max}=h\nu_{max}$) is the maximum of the difference between the glass VDOS and its Debye counterpart. If the linearly dispersing behavior for frequencies lower than ν_{max} definitely assesses the propagation of the considered vibrational modes, the dispersing behavior above ν_{max} should be interpreted with much care, in particular when trying to relate it to the VDOS excess: on the one hand, the modes around the VDOS-EX maximum have a strong *transverse* character[10,11] and therefore lie at lower frequencies than those of the longitudinal modes for a same momentum Q. On the other hand, the apparent dispersion *above* ν_{max} of the longitudinal modes can be explained by the size distribution of nanoheterogeneities.[12] In any case, it is clear that in the spectral range of the VDOS-EX a partial localization of the vibrational modes occurs. The recent reexamination of the IXS data of silica,[13] taking into account a possible scattering from transverse type modes, led to a more complete and open description of this archetype glass. As will be shown in the following, this description is close to support the hereby proposed scenario.

 ©2007 The American Physical Society

The scenario proposed in the present article is based on the idea that the boson peak is a signature of the hybridization of acoustic modes with modes of a localized nature, inherent to the elastic heterogeneities. The relevance of the concept of hybridization in disordered structures was clearly demonstrated in systems where the atoms occupy ideal crystalline positions and are connected by springs having randomly distributed constants.[14] In these systems, it is found that a VDOS-EX appears, originating from the lowest-energy van Hove singularity of the perfect crystal. The crystal lowest-energy acoustic branch is repelled to lower energies because of the disorder-induced hybridization of the acoustic modes with the upper optical branches of the crystal. However, this interpretation is not convincing to justify the VDOS-EX of glasses on a general basis because over distances larger than the interatomic separations, the arrangement of atoms in regular glasses is far from being crystalline.

To support the concept of hybridization with localized modes of elastic nanoheterogeneities in glasses, we believe it is more judicious to compare the vibrational dynamics of glasses with those of nanocluster-based structures, rather than with those of homogeneous crystal-like structures. With this respect, icosahedral quasicrystals like *i*-AlPdMn and *i*-ZnMgY are ideal reference systems as their dynamics feature acoustic-optical hybridizations[15–19] which, in the light of the recently proposed origin of the low frequency hybridizing optical modes,[20] happen to be closely related to the existence of nanometric icosahedral nanoclusters. The relevance of the quasicrystal dynamics to better understand those of glasses is very justified. Indeed, for those metallic alloys that can exist in the three different phases (crystal, icosahedral quasicrystal, and glass), the glassy dynamics were found to be very close to those of the quasicrystalline phase[21] (existence of a VDOS-EX), in addition to structural[22] and thermodynamical[23,24] similarities.

It is the aim of this study to clarify the low-frequency vibrational dynamics in glasses through the comparison with those of quasicrystals. In the following section, we recall the main points of the optical-like low-frequency dynamics of nanometer sized objects and how they relate to nanoheterogeneities in glasses and icosahedral clusters in quasicrystals. Then, on the basis of published experimental data, we present in more details the hybridization schemes of longitudinal and transverse acoustic modes with cluster-type eigenmodes, (i) in *i*-AlPdMn and *i*-ZnMgY quasicrystals (Sec. III A) and (ii) in several glasses (Sec. III B). This interpretation comes out as a refinement of our previously proposed explanations of the VDOS-EX in glasses.[1,12,25]

II. MODEL OF NANOELASTICITY IN GLASSES COMPARED TO THE ATOMIC ARRANGEMENT IN ICOSAHEDRAL QUASICRYSTALS

Over about twenty years, it has been suggested that the vibrations in the spectral range of the VDOS-EX can be identified with the lowest or surface modes of nanoheterogeneities which are intrinsic to the structure of glasses.[1] In the proposed model, the nanoheterogeneities are nanometric more cohesive domains which are separated by softer interfacial zones. It is important to keep in mind that the considered nanoheterogeneities need not be associated with density fluctuations but only with elastic (or cohesion) fluctuations, as recently confirmed by simulation works.[5,6] It is not easy to have a precise idea of the domain shapes which probably change from one type of glass to another, while it is *very* likely that there exists a more or less broad domain size distribution.

The lowest vibration frequencies of a spherical domain with diameter D is given by the following expression:[26–28]

$$\nu_{\ell np} = S_{\ell np}\frac{c_t}{D}, \tag{1}$$

where ℓ is the usual quantum number of spherical harmonics and n the harmonic index, p an index specifying the type of modes, spheroidal or torsional, c_t the transverse sound speed. $S_{\ell np}$ is a coefficient depending on the ℓnp mode and on the ratio c_l/c_t, c_l being the longitudinal sound speed. The lowest frequency of vibration corresponds to the spheroidal quadrupolar $\ell=2$, $n=0$ fundamental mode, for which the coefficient S is close to 0.84, a value that hardly depends on the ratio c_l/c_t. This fundamental quadrupolar mode has a predominant *transverse* character, even if the longitudinal character is not negligible.[29] Obviously, the S coefficient for the lowest-frequency modes depends on the domain shape. Taking into account the shape variation (from cylindrical to spherical), one obtains $0.5<S<0.85$. The mode with a predominant *longitudinal* character, namely the spherical one ($\ell=0, n=0$), has a larger frequency. In fact, the frequencies of the predominantly longitudinal spherical modes are close to those obtained from Eq. (1) replacing c_t with c_l, keeping the same value of $S_{\ell np}$.

The initially proposed model of the nanoscale glass elastic heterogeneity[1] pointed out that one could associate the VDOS-EX peak frequency, ν_{max}, with the lowest-frequency mode of a mean domain size, D_{max}, corresponding to the maximum of a size distribution, so that $\nu_{max}=S(c_t/D_{max})$. The identification with the predominantly transverse modes agrees with the transverse character of the vibrational modes in the boson peak.[10,11] The observed frequencies of VDOS-EX maxima from various glasses lead to domain sizes ranging approximately between 1 nm and 3 nm, depending on the type of glass. The shape of the boson peak was found to be in agreement with a log-normal size distribution.[2,30,31] Note that although Eq. (1) strictly holds for *free* elastic bodies, it was recently shown that it also satisfactorily describes, at least in a first approximation, the cases of embedded clusters, taking into account a weak mechanical coupling between their inside and their surrounding medium.[20] In other words, Eq. (1) is used here as a good evaluation tool of the lowest-frequency modes of elastically (if not structurally) defined nano-objects, expressing the correspondence between the boson peak and the mean size of an elastic heterogeneity.

As mentioned in the introduction, the interpretation of the boson peak through nanometric elastic heterogeneities gets more convincing if one compares the dynamics of glasses to those of quasicrystals. Structural analyses have shown that

the atomic arrangement in icosahedral quasicrystals can be described as a quasiperiodic packing of groups of atoms or "clusters" with a local icosahedral symmetry.[32] Furthermore, it was found that more electrons are localized on clusters than between clusters, supporting this idea of cluster building blocks.[33] Taking into account the existence of such clusters allows to assign a precise origin to the optical nondispersive modes observed through both inelastic neutron scattering (INS) and IXS, in *i*-AlPdMn and *i*-ZnMgY.[15–18] Using Eq. (1), it was found that the lowest-energy optical modes in *i*-AlPdMn and *i*-ZnMgY, except the mode at 7 meV in *i*-AlPdMn and probably also that at 8 meV in *i*-ZnMgY, correspond well to the $\ell=0,1,2$ spheroidal and torsional modes of free continuous nanospheres having the same diameters as the corresponding icosahedral clusters.[20] The good agreement between the experimentally observed frequencies of the optical modes and those calculated from the *free* sphere model means that the matrix-cluster (or cluster-cluster) interface is relatively *soft* and weakens the mechanical coupling between a cluster and its surrounding. More interestingly, computing the cluster mode frequencies starting from a infinite matrix disrupted by a thin spherical shell having *weaker* elastic parameters (thereby defining a spherical cluster) provided a more complete description. This latter picture confirms that a disrupted elastic network, as we claim it is for glasses, generates low lying optical modes that, as will be seen in the following, are likely to hybridize with plane wave acoustic modes. The rather well defined clusters in icosahedral quasicrystals are equivalent to the more cohesive domains in glasses. While in quasicrystals the quasiperiodic packing of coupled clusters is expected to generate coherence among the cluster modes (yet too weak to produce a sizable dispersion of the optical modes), in glasses coherence between domain modes is rather unlikely.

III. HYBRIDIZATION OF ACOUSTIC MODES WITH OPTICAL MODES IN QUASICRYSTALS AND GLASSES

A. Quasicrystals

The hybridization scheme proposed for glasses in the next section is inspired from that observed in icosahedral quasicrystals. The dynamics of the two well known icosahedral quasicrystals, *i*-AlPdMn and *i*-ZnMgY, were extensively studied, using both INS[15,16] and IXS.[17,18]

In both quasicrystals, INS and IXS measurements have identified longitudinal acoustic (LA) and transverse acoustic (TA) modes respectively propagating at c_l and c_t sound speeds (Table I), together with nondispersive optical branches that are consistent with the eigenmodes of the icosahedral clusters, as exposed in the previous section. For both systems, most of these optical branches are seen to merge into early bending portions of the acoustic branches, disclosing hybrizing behaviors. A close examination of the different sets of dispersion curve data (see details in Table I) allow to draw a typical hybridization scheme, schematically drawn in Fig. 1.

The hybridization scenario between acoustic modes and optical cluster modes in quasicrystals is the following. The optical cluster modes display quasihorizontal dispersion curves (considering weak intercluster interaction), lying at frequencies $\approx c_t/D$ and $\approx c_l/D$, according to the previous section. While the lowest energy mode has a strong *transverse* character, the higher energy one has a dominant *longitudinal* character. Hybridizing will occur if the energy of one of these optical modes lies close to that of an acoustic mode. Such situation will naturally occur when the wavelength of the acoustic mode becomes comparable with the cluster size, or as the wave vector of the acoustic mode Q approaches $\frac{2\pi}{D}$, as $\nu_{acoustic}=c\frac{Q}{2\pi}=\frac{c}{D}\approx\nu_{optical}$. Accordingly, a bending of the TA branch is expected at $\left[Q=\frac{2\pi}{D};\nu=\frac{c_t}{D}\right]$ and at $\left[Q=\frac{2\pi}{D};\nu=\frac{c_l}{D}\right]$ for the LA branch. In addition, the LA branch crosses the lowest energy optical branch when $\nu_{LA}=\nu_{optical}^{low}$, i.e.,

TABLE I. Top table: Sound speeds, energy values at bending Q points and energy values of the experimentally observed optical modes together with their dominant transverse (T) or longitudinal (L) character according to the comparison with computed cluster modes (Refs. 20 and 29) in *i*-AlPdMn (Refs. 15, 17, 19, 34, and 35) and *i*-ZnMgY (Refs. 16 and 18). Bottom table: Cluster sizes D and selected wave vector Q values, relevant to the hybridization scheme of *i*-AlPdMn and *i*-ZnMgY.

	c_l (m/s)	c_t (m/s)	$E(Q_{bend}^{TA})$ (meV)	$E(Q_{bend}^{LA})$ (meV)	$E_{optical}^{exp}$ (meV)
					7[b,c]
AlPdMn	6500[a]	3500[a]	12[b–d]	12[c,d]	12[b–d] (T)
				>16[c,d]	16[b,c] (T)
					24[b,c] (L)
					8[e]
ZnMgY	4800[e]	3100[e]	11[f]	≃11[f]	12[e] (T)
				15[e]	17[e] (L)
	D (nm)	Q_{bend}^{TA} (nm^{-1})	Q_{bend}^{LA} (nm^{-1})	$\frac{2\pi}{D}$ (nm^{-1})	$\frac{c_t}{c_l}\frac{2\pi}{D}$ (nm^{-1})
AlPdMn	1[b,g]	6[b–d]		6.3	
			3[c,d]		3.2
ZnMgY	1[f,h]	6[e]	6[f]	6.3	
			4[f]		4

[a]From Ref. 34.
[b]From Ref. 15.
[c]From Ref. 35.
[d]From Ref. 17.
[e]From Ref. 16.
[f]From Ref. 18.
[g]From Ref. 19.
[h]Note that in the present table, the energies of the optical modes for *i*-ZnMgY were computed taking $D=1$ nm, at variance with Ref. 20 where a value of $D=1.2$ nm was taken. To the authors' knowledge, there is no clear justification for this latter value of D in *i*-ZnMgY (Ref. 16). Taking $D=1$ nm leads to the same interpretation of the optical modes as in *i*-AlPdMn, i.e., the lowest energy mode at ≃8 meV (7 meV in *i*-AlPdMn) is ascribed to a cluster/matrix "rattling" mode (Ref. 28).

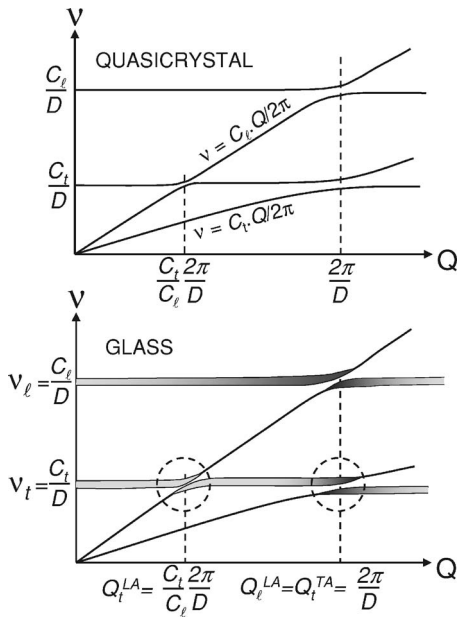

FIG. 1. Typical hybridization scheme in (top panel) quasicrystals (bottom panel) glasses. In the glass case, circles indicate the hybridizing points relevant to the VDOS-EX. The energy width of the pseudo-optical branch qualitatively accounts for the domain size distribution and for the lifetimes of the phonons localized around the domains. The darkness increases with the amplitude of the Fourier components.

when $c_l\frac{Q}{2\pi} \approx \frac{c_t}{D}$, that is at $Q = \frac{c_t}{c_l}\frac{2\pi}{D}$. While the former type of hybridization is most efficient since it couples modes with identical transverse or longitudinal characters, the latter one, relevant to the LA mode only, is expected to be less efficient since it mixes a longitudinal acoustic mode with a predominantly transverse optical mode. However, because of the nonnegligible longitudinal component of the predominantly transverse optical mode, this second type of hybridization may well be observed.

The validity of this hybridizing scheme can be verified from the experimental data of *i*-AlPdMn and *i*-ZnMgY (Table I). In the case of *i*-AlPdMn, a strong bending of the TA dispersion curve was observed[17] at $Q_{bend}^{TA} \approx 6$ nm^{-1}. Energywise, this bending occurs close to the nondispersive optical branch at 12 meV, a value which corresponds to the lowest energy dominantly *transverse* cluster mode in *i*-AlPdMn.[20] In agreement with the hybridization scenario, the Q value at which the bending of the TA branch occurs, $Q_{bend}^{TA} \simeq 6$ nm^{-1}, matches the cluster wave vector value $\frac{2\pi}{D} = 6.3$ nm^{-1}; this bending is consistent with the fact that the TA mode hybridizes with a predominantly *transverse* optical mode. Hybridization of this same optical mode with the LA branch is also observed, as testified by the bending of the LA dispersion curve at ~12 meV from $Q_{bend}^{LA} \approx 3$ nm^{-1}. There again, this latter Q value matches that deduced from $Q = \frac{c_t}{c_l}\frac{2\pi}{D} = 3.4$ nm^{-1}. However, in this case, the observed strong bending of the LA dispersion may also result from strong repelling by the higher optical cluster mode, lying at 16 meV,[20] i.e., not far above 12 meV. Finally, it is noted that no hybridization of any acoustic branch with the lowest energy optical branch at 7 meV was observed. The nature of this very low energy mode, identified as a cluster/matrix mode ("rattling" motion of the cluster in the matrix[20]), may be at the origin of its very weak coupling with the acoustic dynamics.

The observed behavior of the acoustic branches is not very different in *i*-ZnMgY. A strong bending is observed[16,18] for the TA branch at $Q_{bend}^{TA} \approx 6$ nm$^{-1} \simeq \frac{2\pi}{D}$. This bending corresponds to the crossing of the TA branch with the optical branch lying at ≈11 meV; this branch can be identified with the cluster mode with frequency $\sim\frac{c_t}{D}$. Like in *i*-AlPdMn, a hybridization of the LA modes with the same optical modes at ≈11 meV can be deduced from the IXS experimental results[18] at $Q_{bend}^{LA} \approx 4$ nm^{-1}. As expected, this value of Q is close to $\frac{c_t}{c_l}\frac{2\pi}{D}$. Furthermore, the phonon dispersion obtained by IXS[18] is compatible with a hybridization of the LA modes with the nondispersive optical modes at ≈17 meV corresponding to the frequency $\approx\frac{c_l}{D}$. Similarly to *i*-AlPdMn, no hybridization is apparent with the lowest optical modes at 8 meV.[16,18]

The hybridization scheme in *i*-AlPdMn and *i*-ZnMgY appears all the more obvious as experiments allow to identify it quite unambiguously. Accordingly, both optical modes and flattening portions of the dispersion curves give rise to pile-ups in the VDOS, showing up as strong peaks or at least deviations from the Debye VDOS.[36,37] The observability of the optical modes in the dispersion curves is most probably due to the relatively long range coherence between the cluster modes. As the coherence length is reduced, this observability is expected to be reduced but the hybridizing scenario remains valid. This is precisely what we expect to occur in the case of glasses.

B. Hybridization of acoustic modes with optical-like (domain) modes in glasses

1. General description

The correspondence between quasicrytals and glasses is straighforward for the metallic compounds that can exist in either of the glassy or quasicrystal phases. As recalled in the Introduction, a very similar VDOS-EX was found in the case of the glass-forming Pd-Si-U alloy:[21] subtracting the VDOS of the Pd-Si-U crystalline phase from that of its glassy phase or that of its quasicrystal phase evidences an excess of modes at low energy. This VDOS-EX can reasonably be associated with the existence of a nanometric heterogeneity, the main difference between the two phases lying in the arrangement of local clusters over supercluster distances: while it is more ordered in the quasicrystalline phase, it is expected to be disordered in the metallic glassy phase. This VDOS-EX was found to be larger in the glass/crystal difference than in the quasicrystal/crystal difference. More interestingly, it was observed that the VDOS-EX of the glass decreased as the glass was annealed (or "relaxed"[21]), yet remaining above that of the quasicrystal. This behavior is very similar to the behavior observed for regular glasses.[38,39] With this respect, the lowest VDOS-EX observed in the quasicrystal case identifies it as "super-aged" metallic glass: the lower the VDOS-EX, the

smoother the elastic nanometric heterogeneity.[39]

On the grounds that the existence of nanometric clusters is a determining factor for the low energy dynamics of either an icosahedral quasicrystal or that of its glass counterpart, we suggest that more cohesive nanodomains in glasses play the same role as the icosahedral clusters in quasicrystals or glassy metals. Obviously, in most glasses, the atomic organization in the cohesive nanodomains is not icosahedral, especially in organic or polymeric glasses. However, once again, the atomic arrangement within the domains is less important than the *elastic* fluctuations associated with the domains' cohesion. Similarly to the case of quasicrystals, optical-like modes of the cohesive nanodomains coexist with longitudinal and transverse acoustic modes, so that hybridizations of acoustic modes with nanodomain modes are expected. Figure 1 illustrates the typical hybridization scheme in glasses. The main difference with that of quasicrystals is that the optical-like modes in glasses are expected to have energies distributed over a larger spectral range than do those of clusters in quasicrystals because of relatively large size and shape distributions. Instead of true optical modes like in quasicrystals, the optical-like modes in glasses should rather be considered as the localized lowest-frequency modes of the cohesive domains. The Fourier decomposition of a vibration mode localized at the surface of a domain of size D is expected to present a maximum at the wave vector $Q=\frac{2\pi}{D}$ and a width $\approx Q$. As mentioned earlier, long range quasiperiodic arrangements of domains in glasses are unlikely, at variance with icosahedral clusters in quasicrystals.

As the shape of the cohesive domains is in general not known, no precise prediction can be done about the exact value of the S coefficient in Eq. (1), except that $0.5 \leqslant S \leqslant 1$. For this reason, and along the notations used for quasicrystals, the frequency of the predominantly *longitudinal* lowest-frequency domain mode is simply written as $\nu_l \simeq \frac{c_l}{D}$ and that of the predominantly *transverse* one, $\nu_t \simeq \frac{c_t}{D}$, D being considered as an effective domain size. Similarly to quasicrystals, the LA branch will hybridize with the predominantly *longitudinal* domain mode at $\left[Q_l^{LA}=\frac{2\pi}{D};\nu_l^{LA}=\frac{c_l}{D}\right]$ while the TA branch will hybridize with the predominantly *transverse* domain mode at $\left[Q_t^{TA}=\frac{2\pi}{D};\nu_t^{LA}=\frac{c_t}{D}\right]$. Moreover, the LA branch will hybridize, though less efficiently, with the predominantly *transverse* domain mode at $\left[Q_t^{LA}=\frac{c_t}{c_l}\frac{2\pi}{D};\nu_t^{LA}=\frac{c_t}{D}\right]$. The hybridization between these different branches, associated with local bendings of the dispersion curves around Q_t^{LA} and Q_t^{TA}, inevitably generates mode accumulations at the corresponding hybridizing energies, i.e., an *excess* of VDOS with respect to that of a homogeneous medium. As the main Q component of the domain mode lies at $\frac{2\pi}{D}$, the VDOS-EX is due mainly to the hybridization of the TA modes with the lowest-frequency modes of the cohesive domains and only partially to the hybridization of the LA modes with these same lowest-frequency modes.

The energy position of the hybridization induced VDOS-EX is expected to compare with the maximum of the *difference* between the glass VDOS and its Debye counterpart (E_{max}). This maximum shall not be mistaken for the one observed in the case of a crystal VDOS, which lies at definitely larger energies than that of the boson peak, as mentioned in the Introduction. Obviously, the maximum of the difference between a crystal VDOS and its Debye counterpart corresponds to the van Hove singularities inherent to the crystalline phonon dispersion curves. The use of E_{max}, instead of E_{DOS}, was already discussed[40] and is still under debate. The maximum of the *difference* (E_{max}) is preferred to the *ratio* (E_{DOS}) because in the case of the ratio the $1/\omega^2$ factor shifts artificially considerably the energy position of the "excess" modes to low energies. As for Raman scattering, quite logically [considering the almost linear variation of the light coupling coefficient $C(E)$], one observes that the Raman boson peak energy, E_{BP}, defined as the maximum of the Stokes intensity divided by $[E(n(E)+1)]$ [where $n(E)$ is the Bose factor], lies, for many glasses, about half way between E_{DOS} and E_{max}. Finally, note that in any case no perfect correspondence is to be expected between the hybridizing energies and the values of E_{max}, all the more so as the dispersion curves of glasses determined by IXS feature nonnegligible error bars.

Another way of expressing the hybridization between the optical-like domain modes and the acoustic branches is to write that the wavelength of the TA modes involved in the VDOS-EX is $\lambda_T \simeq D$, and that of the LA modes $\lambda_L \simeq D(c_l/c_t)$. Finally, it is obtained for the frequency of the VDOS-EX maximum:

$$\nu_{max} \simeq \frac{c_t}{\lambda_T} = \frac{c_l}{\lambda_L}. \tag{2}$$

This same result was derived from numerical simulation analyses.[6]

Finally, note that because of the size distribution of domains, the observed frequency and Q values will reflect hybridizations with the mean domain size D_{max} (for clarity, the subsequent notations referring to the glass parameters will omit the "*max*" subscript).

2. $(Li_2O)_{0.5}B_2O_3$ *glass*

To illustrate the applicability of this hybridizing scheme, we first consider the case of $(Li_2O)_{0.5}B_2O_3$ glass, for which rather precise IXS analyses have been reported. At this stage, it should be stressed that the IXS expriments performed on glasses essentially probe the LA dynamics, and only very rarely may the TA components be observed.[13,41] Therefore, the hybridizing behavior of the transverse dynamics, which, according to the presented model, is at the origin of the VDOS-EX in glasses, can only be inferred from that of the longitudinal dynamics.

Two series of IXS measurements were carried out on $(Li_2O)_{0.5}B_2O_3$. The first one was performed by Matic *et al.*,[9] and the second very recent one was reported by Rufflé *et al.*[42] While the data of the former study cover a wide Q range ($0-12$ nm^{-1}), those of the second study essentially focus on the Q region below 3 nm^{-1}, with enhanced data accuracy. As shown below, these two data sets provide a very complete and consistent picture of the hybridizing dynamics in $(Li_2O)_{0.5}B_2O_3$.

In the Matic *et al.* experiment,[9] the longitudinal acoustic

TABLE II. Hybridizing Q and E values as read from published IXS and Brillouin light scattering data on $(Li_2O)_{0.5}B_2O_3$, B_2O_3, and d-SiO_2. The last column indicates the energies of the boson peaks in the respective glasses. The agreement between the different ratios (sound speeds, wave vectors, and energies) supports the hybridization scenario.

	c_l (m/s)	c_t (m/s)	$\frac{c_t}{c_l}$	Q_l^{LA} (nm^{-1})	Q_t^{LA} (nm^{-1})	$\frac{Q_t^{LA}}{Q_l^{LA}}$	E_l^{LA} (meV)	E_t^{LA} (meV)	$\frac{E_l^{LA}}{E_t^{LA}}$	E_{max} (meV)	E_{BP} (meV)	E_{DOS} (meV)
$(Li_2O)_{0.5}B_2O_3$	6700[a]	3700[a]	0.55	4[b]	~2.1[c]	~0.53	16[b]	9[c]	0.56		9[a]	
B_2O_3	3300[a]	1900[a]	0.58	2.5[d]			5.5[d]			3.75[e]	3[a]	2.2[e]
d-SiO_2			0.63[f]	(3.5)[g]	2.2[h]	0.63		9[h]		11[i]	9[j]	7.7[k]

[a]From Ref. 43.
[b]From Ref. 9.
[c]From Ref. 42.
[d]From Ref. 44.
[e]From Ref. 45 and see Fig. 2.
[f]This value is assumed to be identical to that in v-SiO_2 (see text).
[g]This value was inferred from the IXS data of v-SiO_2 (Ref. 8), on the grounds that the domain sizes in d-SiO_2 and v-SiO_2 are identical (see text).
[h]From Refs. 46–48.
[i]From Ref. 48.
[j]From Ref. 49.
[k]From Ref. 50.

dispersion is found to display a *major* bending from $Q \simeq 4$ nm^{-1} with an energy flattening value of $E \simeq 16$ meV. In the Rufflé *et al.* experiment,[42] the more salient result is an *inflection* of the LA dispersion curve from $Q \simeq 2$ nm^{-1} ($E \simeq 9$ meV), mostly obvious in the Q dependence of the width of the inelastic excitations and interpretated as a Ioffe-Regel like crossover from propagating to nonpropagating LA modes in the interval $2 < Q$ $(nm^{-1}) < 2.5$ and at $E \simeq 9$ meV.

Within the proposed hybridization scheme, the strong bending of the LA dispersion curve[9] corresponds to the hybridization of the LA branch with the predominantly *longitudinal* domain mode, i.e., $Q_l^{LA} \simeq 4$ nm^{-1} and $E(Q_l^{LA}) \simeq 16$ meV. Having $Q_l^{LA} = \frac{2\pi}{D}$, one obtains $D \simeq 1.6$ nm. Using the measured sound velocities[43] (Table II) the energy of the predominantly *longitudinal* domain mode is $E_l = h\nu_l = h\frac{c_l}{D} \simeq 17$ meV. This latter value is very close to the IXS experimental value $E(Q_l^{LA})$. The Ioffe-Regel-like crossover[42] detected around 2.1 nm^{-1} should be associated with the hybridization of the LA branch with the predominantly *transverse* domain mode, so that $Q_t^{LA} = 2.1$ nm^{-1} (note that the weakness of the inflection of the LA dispersion curve observed at this Q point[42] is consistent with the poor hybridizing efficiency between modes with different polarizations). This value agrees with that decuded from $\frac{2\pi}{D}\frac{c_t}{c_l} = 2.2$ nm^{-1}. It is very remarkable to find that, from the experiment,[9,42] $\nu_t/\nu_l = 0.56 \simeq c_t/c_l$ and $Q_t^{LA}/Q_l^{LA} \simeq 0.55 \simeq c_t/c_l$. These results strongly sustain the proposed model.

As already noted, the IXS experiments allow to probe essentially the longitudinal acoustic dynamics, while the VDOS-EX or the Raman boson peak have proved to feature a dominant transverse character.[10,11] Accordingly, the origin of the VDOS-EX shall be searched in the *transverse* dynamics. The strongest hybridization involving the transverse dynamics is that mixing the TA branch with the dominantly *transverse* domain mode, occurring at $Q_t^{TA} = Q_l^{LA} = \frac{2\pi}{D}$ and $E_t^{TA} = E_t = h\frac{c_t}{D} \simeq 9.6$ meV. This value lies very close to that obtained from the hybridization of the LA branch with the dominantly *transverse* domain mode, E_t^{LA}.

It is expected that the energies, E_t^{TA} and E_t^{LA}, approximately correspond to the energy of the VDOS-EX maximum, E_{max}. The measurement of the VDOS in $(Li_2O)_{0.5}B_2O_3$ has not been reported so far. However, the Raman boson peak was measured; it was found to be $E_{BP} = 9$ meV.[43] As discussed above, E_{BP} may be used as an underestimated value of E_{max}, so that one can conclude to a fair agreement between the hybridizing energies (E_t^{TA}, E_t^{LA}) and the maximum of the VDOS-EX, E_{max}.

The fact that $\lambda_L \simeq 1.8D$ indicates that $\nu_{max} \approx \nu_{co}$, ν_{co} being the frequency at the Ioffe-Regel-like crossover, as found from experiment.[42] Overall, one notices that depending on the analysis performed of the IXS data, complementary information on the hybridization scheme are obtained. An analysis performed in terms of plain propagating dynamics (using a damped harmonic oscillator for instance) will tend to locate the strong bending of the LA dispersion curve, due to its hybridization with the predominantly *longitudinal* domain modes. Meanwhile, a Ioffe-Regel-like analysis will disclose the crossover point (Fig. 1) in the LA dispersion curve, that corresponds to the hybridization of the LA branch with the predominantly *transverse* domain modes.

3. B_2O_3 *glass*

The interpretation of the VDOS-EX for the $(Li_2O)_{0.5}B_2O_3$ glass is likely to be transposable to most of glasses. For example, in the case of the B_2O_3 glass[44] (Table II) the LA dispersion curve bends to become almost horizontal at $Q_l^{LA} \simeq 2.5$ nm^{-1} and $E_l^{LA} \simeq 5.5$ meV. As, for this glass, $c_l = 3300$ m/s and $c_t = 1900$ m/s,[43] one deduces that the mixing

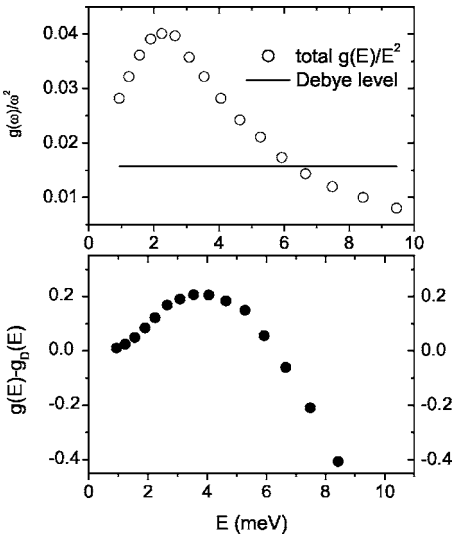

FIG. 2. Top panel: VDOS excess (E_{DOS}) of B_2O_3 as displayed by $g(E)/E^2$, together with the Debye level [data of Engberg *et al.* (Ref. 45)]. Bottom panel: VDOS excess (E_{max}) defined by the *difference* between $g(E)$ and the Debye density of states $g_D(E)$.

point of the TA modes with the lowest-frequency domain modes lies at $Q_t^{TA}=Q_l^{LA}\simeq 2.5$ nm^{-1} and $E_t^{TA}=\hbar c_t Q_t^{TA}\simeq 3$ meV. Unlike $(Li_2O)_{0.5}B_2O_3$, the value of E_{max} for this glass can be deduced from INS measurements[45] (see Fig. 2). One finds $E_{max}\approx 3.75$ meV, a value slightly larger than $E_{BP}\simeq 3$ meV.[43] It is noted that the value of 3.75 meV found for E_{max} is exactly that deduced by Yannopoulos *et al.*[40] from the same experimental data.[45]

There again, the fair agreement between E_t^{TA} and E_{max} supports the hybridizing scenario for this glass. From Q at the bending of the LA branch, one deduces that the mean domain size in the B_2O_3 glass is $D\simeq 2.5$ nm. A same value of D was deduced from the first sharp diffraction peak.[51]

4. SiO_2 *glass*

The experimental results obtained by IXS on glassy silica,[8,52] which have been much debated, are interesting from the viewpoint presented in this paper. The case of normal vitreous silica (v-SiO_2) is better understood by examining in the first place that of densified silica (d-SiO_2), for which the elastic constants are stronger and thus less ambiguously extracted from the IXS data.

In the case of d-SiO_2 (density $\rho=2.62$ g/cm^3), a Ioffe-Regel-like analysis led to the determination of a crossover wave vector $Q_{co}\simeq 2.2$ nm^{-1}, associated with the crossover energy $E_{co}\simeq 9$ meV.[47] According to the hybdridization scheme, these two values respectively correspond to Q_l^{LA} and E_t^{LA}, referring to the hybridization of the LA branch with the predominantly *transverse* domain modes. Although this latter hybridization is not expected to bring the main contribution to the VDOS-EX, as previously explained, nevertheless it allows to verify that the value $E_t^{LA}\simeq 9$ meV is correlated to that of E_{max}. From the VDOS determined by INS (Ref. 50) and the Debye one, it was obtained[48] $E_{max}\simeq 11$ meV. Furthermore, like for the two already considered glasses, $E_t^{LA}\simeq E_{BP}$: from Raman scattering[49] $E_{BP}\simeq 9$ meV. The mean size of domain in d-SiO_2 is given by $D\simeq\frac{2\pi}{Q_t^{LA}}\frac{c_t}{c_l}$. It is reasonable to assume that the ratio $\frac{c_t}{c_l}\simeq 0.63$ remains unchanged from nondensified silica to densified silica, so that $D\simeq 1.8$ nm.

Dealing now with the case of normal v-SiO_2, the extraction of the Q_t^{LA} and E_t^{LA} values from the IXS data through a Ioffe-Regel-like analysis becomes very uncertain because of too low crossover wave vector and energy values.[49] The results obtained from the propagating dynamics analysis performed by Benassi *et al.*[8] still allows to draw a consistent picture of the hybridization scheme in v-SiO_2. In this study, the dispersing behavior of the LA branch is found to end at about 3.5 nm^{-1}. This Q point should be identified with the hybridization point between the LA branch and the predominantly *longitudinal* domain mode, occurring at Q_l^{LA}. The mean domain size obtained from this value is $D=\frac{2\pi}{Q_l^{LA}}\simeq 1.8$ nm, i.e., a value identical to that found for d-SiO_2. Following the suggestion of Sokolov *et al.*,[53] that the width of the first sharp diffraction peak (FSDP) is inversely proportional to D, the no-change of D is confirmed by the observed no-change of the FSDP width with the SiO_2 density.[54] Furthermore, this result meets the conclusions drawn from simulation works,[6] according to which the size D of elastic nanoheterogeneities remains unmodified upon densification.

Following the hybridization scenario, one obtains for the energy of the predominantly *transverse* domain mode in v-SiO_2 $E_t^{TA}=hc_t\frac{Q_t^{LA}}{2\pi}=hc_l\frac{c_t}{c_l}\frac{Q_t^{LA}}{2\pi}\simeq 8.4$ meV (taking $c_l=5800$ M/s). This value is in agreement with the early found value of E_{max} in v-SiO_2,[55] $E_{max}\simeq 8.2$ meV.

5. *Boson peak, phonon dispersion, and glass-network elasticity*

As observed by IXS, the phonon dispersion curves of some glasses are almost linear, without visible bending in the first Brillouin pseudozone (yet still with a rapid broadening of the excitations upon Q increase) up to about $Q_p/2$, Q_p being the momentum of the FSDP peak. This was clearly observed for an ionic glass, $Ca_{0.4}K_{0.6}(N0_3)_{1.4}$ (CKN),[44] and molecular glasses like propylene carbonate[56] and o-terphenyl[57] and less clearly for polybutadiene.[58] Considering the fragility index of these glasses (according to the classification of Angell[3]), one is tempted to relate this behavior to the "fragile" aspect of these glasses.

According to the nanoheterogeneity picture such observation can be explained by the fact that in these glasses the elastic constant contrast between cohesive domains and softer interfacial zones is much weaker than in "strong glasses." As a consequence, the hybridization between acoustic modes and the poorly defined localized vibrational modes of nanodomains is less relevant, giving rise to a weak VDOS-EX. In other words, a quasilinear phonon dispersion through the entire first Brillouin pseudozone is related to a weak boson peak.

The relation between a weak boson peak, a weak amplitude of elastic constant fluctuations and fragility, was underlined in very recent papers.[59,60] According to Ref. 60, the physical property which is decisive for the amplitude of VDOS-EX or of the boson peak, i.e., for the efficiency of the

hybridization between acoustic modes and localized domain modes, is the nanometric-scale fluctuating glass-network cohesion. As a matter of fact, the as-defined fragility[3] does not depend only on the glass-network elasticity. More precisely, Novikov *et al.*[60] showed that there is a linear dependence, on the one hand, between the fragility index and the ratio $(c_l/c_t)^2$, on the other hand, between the amplitude of the boson peak and the same ratio $(c_l/c_t)^2$. An exception was underlined for some glasses like lithium borates, in which Li^+ ions have a very weak effect on the c_l/c_t ratio but not on the fragility index.[60] These glasses have a rather strong network [low (c_l/c_t)], but they are relatively fragile. The fragility of these glass-forming liquids is mainly due to the Li^+ motion. The fluctuating glass cohesion is precisely characterized by the ratio c_l/c_t, the smaller c_l/c_t ratio the stronger fluctuating cohesion.[60] The respective ratios c_l/c_t of $(Li_2O)_{0.5}B_2O_3$ glass $(c_l/c_t \simeq 1.8)$ and CKN glass $(c_l/c_t \simeq 2.2)$ allow to justify why in the former case the boson peak, and therefore the hybridization, is stronger. From these remarks, one concludes that it is the glass network elasticity characterized by the c_l/c_t ratio, which is generally decisive for the efficiency of the hybridization between acoustic and localized modes and for the amplitude of the boson peak, rather than the fragility index. This conclusion meets that of Matic *et al.*[44] in the sense that the observation of a bending in the dispersion curves is related to the glassy network.

Along the previous considerations, the case of ethanol must be raised. A relatively strong boson peak was observed for the structural glassy phase[61] while the phonon dispersion curve of this glassy phase, as observed by IXS,[62] is close to that of the monoclinic crystal. This similarity is not in contradiction with the proposed model (Fig. 1). However, from the amplitude of the boson peak one should expect a bending in the IXS dispersion of the glassy phase, associated to the hybridization. Such was not confirmed by the experiment. Unfortunately, the value of c_t, and therefore the c_l/c_t ratio of this glass has not yet been determined. The case of ethanol should deserve a more detailed experimental study before going further in the interpretation.

IV. SUMMARY

Unlike continuous elastic media, the phonon dispersion curves (and the related elastic quantities like the vibrational density of states) in nanometrically heterogeneous solids are expected to feature peculiarities due to hybridizing dynamics.

Nanometric heterogeneities, or clusters, exist in icosahedral quasicrystals. In the quasicrystalline phase, that is closer to the glassy phase than to the crystalline one, the clusters are likely to form a quasiperiodic organization. In consequence, optical vibration modes appear as combinations of cluster internal modes. Because the coupling between clusters is weak, these optical modes are apparently nondispersive. The crossings of the longitudinal and transverse acoustic branches with the lowest nondispersive optical modes, also observed by IXS and INS at different exchanged energies and momenta, induce a hybridization between acoustic and optical modes.

In glasses, optical-like modes are identified with the modes localized at the surface of elastic nanoheterogeneities whose long postulated existence[1] was recently unveiled by numerical simulation.[5–7] Although no quasiperiodic arrangement of nanodomains has been demonstrated up to now, the comparison of the inelastic scattering data from glasses with those from quasicrystals is helpful because of the more contrasted nanometric structure of quasicrystals. Even in the absence of domain quasiperiodicity in glasses, the domain modes can hybridize with the LA and TA modes at different wave vectors Q because the localized waves Fourier transform into different propagating waves corresponding to different wave vectors. According to this hybridization scheme, the domain lowest-frequency modes hybridize with the LA modes and the TA modes at about the same frequency, that corresponds to the VDOS-EX maximum frequency. As observed by simulation and experiment, the low-frequency acoustic modes in the boson peak have a marked *transverse* character. It is why one concludes that the VDOS-EX is mainly due to the hybridization of the TA modes with the predominantly *transverse* domain surface modes.

The comparison of the low-frequency vibrational dynamics in glasses and in icosahedral quasicrystals turns out to be helpful in finding a consistent interpretation of the VDOS-EX or of the boson peak in glasses. The different IXS results, which had long seemed contradictory become now complementary. The principal interest of this work is to have shown that the VDOS-EX can well be connected to the hybridization of longitudinal and transverse acoustic modes with the surface lowest-frequency modes of cohesive nanodomains which exist in glasses. This idea of hybridization of propagating modes with localized modes was recently suggested for densified silica.[48] In this paper, it is shown that the localized modes are vibration modes of nanometric heterogeneities.

[1] E. Duval, A. Boukenter, and T. Achibat, J. Phys.: Condens. Matter **2**, 10227 (1990).
[2] A. Mermet, N. V. Surovtsev, E. Duval, J. F. Jal, and J. Dupuy-Philon, Europhys. Lett. **36**, 277 (1996).
[3] C. A. Angell, J. Non-Cryst. Solids **73**, 1 (1985).
[4] H. Sillescu, J. Non-Cryst. Solids **243**, 81 (1999).
[5] B. Rossi, G. Viliani, E. Duval, L. Angelani, and W. Garber, Europhys. Lett. **71**, 256 (2005).
[6] F. Léonforte, R. Boissière, A. Tanguy, J. P. Wittmer, and J. L. Barrat, Phys. Rev. B **72**, 224206 (2005).
[7] F. Léonforte, A. Tanguy, J. P. Wittmer, and J. L. Barrat, Phys. Rev. Lett. **97**, 055501 (2006).
[8] P. Benassi, M. Krisch, C. Masciovecchio, V. Mazzacurati, G. Monaco, G. Ruocco, F. Sette, and R. Verbeni, Phys. Rev. Lett.

77, 3835 (1996).
[9] A. Matic, D. Engberg, C. Masciovecchio, and L. Börjesson, Phys. Rev. Lett. **86**, 3803 (2001).
[10] M. T. Dove, M. J. Harris, A. C. Hannon, J. M. Parker, I. P. Swainson, and M. Gambhir, Phys. Rev. Lett. **78**, 1070 (1997).
[11] V. N. Novikov, E. Duval, A. Kisliuk, and A. P. Sokolov, J. Chem. Phys. **102**, 4691 (1995).
[12] E. Duval and A. Mermet, Phys. Rev. B **58**, 8159 (1998).
[13] B. Ruzicka, T. Scopigno, S. Caponi, A. Fontana, O. Pilla, P. Giura, G. Monaco, E. Pontecorvo, G. Ruocco, and F. Sette, Phys. Rev. B **69**, 100201(R) (2004).
[14] S. N. Taraskin, Y. L. Loh, G. Natarajan, and S. R. Elliott, Phys. Rev. Lett. **86**, 1255 (2001).
[15] M. Boudard, M. de Boissieu, S. Kycia, A. I. Goldman, B. Hennion, R. Bellissent, M. Quilichini, R. Currat, and C. Janot, J. Phys.: Condens. Matter **7**, 7299 (1995).
[16] K. Shibata, R. Currat, M. de Boissieu, T. J. Sato, H. Takakura, and A. P. Tsai, J. Phys.: Condens. Matter **14**, 1847 (2002).
[17] M. Krisch, R. A. Brand, M. Chernikov, and H. R. Ott, Phys. Rev. B **65**, 134201 (2002).
[18] R. A. Brand, J. Voss, F. Hippert, M. Krisch, R. Sterzel, W. Assmus, and I. R. Fisher, J. Non-Cryst. Solids **334-335**, 207 (2004).
[19] M. de Boissieu, R. Currat, S. Francoual, and E. Kats, Phys. Rev. B **69**, 054205 (2004).
[20] E. Duval, L. Saviot, A. Mermet, and D. B. Murray, J. Phys.: Condens. Matter **17**, 3559 (2005).
[21] J. B. Suck, H. Bretscher, H. Rudin, P. Grütter, and H. J. Güntherodt, Phys. Rev. Lett. **59**, 102 (1987).
[22] J. L. Robertson, S. C. Moss, and K. G. Kreider, Phys. Rev. Lett. **60**, 2062 (1988).
[23] L. C. Chen, F. Spaepen, J. L. Robertson, S. C. Moss, and K. Hiraga, J. Mater. Res. **5**, 1871 (1990).
[24] K. F. Kelton, J. Non-Cryst. Solids **334-335**, 253 (2004).
[25] E. Duval, A. Mermet, R. L. Parc, and B. Champagnon, Philos. Mag. **84**, 1433 (2004).
[26] H. Lamb, Proc. London Math. Soc. **13**, 187 (1882).
[27] E. Duval, A. Boukenter, and B. Champagnon, Phys. Rev. Lett. **56**, 2052 (1986).
[28] D. B. Murray and L. Saviot, Phys. Rev. B **69**, 094305 (2004).
[29] L. Saviot and D. B. Murray, Phys. Rev. B **72**, 205433 (2005).
[30] V. K. Malinovsky, V. Novikov, and A. P. Sokolov, Phys. Lett. A **153**, 63 (1991).
[31] T. Pang, Phys. Rev. B **45**, 2490 (1992).
[32] C. Janot, *Quasicrystals: A Primer*, 2nd ed. (Oxford University Press, Cambridge, 1994).
[33] K. Kirihara, T. Nagata, K. Kimura, K. Kato, M. Takata, E. Nishibori, and M. Sakata, Phys. Rev. B **68**, 014205 (2003).
[34] Y. Amazit, M. de Boissieu, and A. Zarembovitch, Europhys. Lett. **20**, 703 (1992).
[35] M. de Boissieu, M. Boudard, R. Bellissent, M. Quilichini, B. Hennion, R. Currat, A. I. Goldman, and C. Janot, J. Phys.: Condens. Matter **5**, 4945 (1993).
[36] M. Scheffer and J. B. Suck, J. Alloys Compd. **342**, 310 (2002).
[37] J. B. Suck and M. Scheffer, J. Non-Cryst. Solids **334-335**, 291 (2004).
[38] C. Angell, Y. Yue, L. Wang, J. Copley, S. Borick, and S. Mossa, J. Phys.: Condens. Matter **15**, 1 (2003).
[39] E. Duval, L. Saviot, L. David, S. Etienne, and J. F. Jal, Europhys. Lett. **63**, 778 (2003).
[40] S. N. Yannopoulos, K. S. Andrikopoulos, and G. Ruocco, J. Non-Cryst. Solids **352**, 4541 (2006).
[41] T. Scopigno, E. Pontecorvo, R. D. Leonardo, M. Krisch, G. Monaco, G. Ruocco, B. Ruzicka, and F. Sette, J. Phys.: Condens. Matter **15**, S1269 (2003).
[42] B. Rufflé, G. Guimbretière, E. Courtens, R. Vacher, and G. Monaco, Phys. Rev. Lett. **96**, 045502 (2006).
[43] J. Lorösch, M. Couzi, J. Pelous, R. Vacher, and A. Levasseur, J. Non-Cryst. Solids **69**, 1 (1984).
[44] A. Matic, L. Börjesson, G. Ruocco, C. Masciovecchio, A. Mermet, F. Sette, and R. Verbeni, Europhys. Lett. **54**, 77 (2001).
[45] D. Engberg, A. Wischnewski, U. Buchenau, L. Börjesson, A. J. Dianoux, A. P. Sokolov, and L. M. Torell, Phys. Rev. B **58**, 9087 (1998).
[46] E. Rat, M. Foret, E. Courtens, R. Vacher, and M. Arai, Phys. Rev. Lett. **83**, 1355 (1999).
[47] M. Foret, R. Vacher, E. Courtens, and G. Monaco, Phys. Rev. B **66**, 024204 (2002).
[48] B. Rufflé, M. Foret, E. Courtens, R. Vacher, and G. Monaco, Phys. Rev. Lett. **90**, 095502 (2003).
[49] E. Courtens, M. Foret, B. Hehlen, B. Rufflé, and R. Vacher, J. Phys.: Condens. Matter **15**, 1281 (2003).
[50] Y. Inamura, M. Arai, O. Yamamuro, A. Inaba, N. Kitamura, T. Otomo, T. Matsuo, S. M. Bennington, and A. C. Hannon, Physica B **263-264**, 299 (1999).
[51] L. Börjesson, A. K. Hassan, J. Swenson, L. M. Torell, and A. Fontana, Phys. Rev. Lett. **70**, 1275 (1993).
[52] M. Foret, E. Courtens, R. Vacher, and J. B. Suck, Phys. Rev. Lett. **77**, 3831 (1996).
[53] A. P. Sokolov, A. Kisliuk, M. Soltwisch, and D. Quitmann, Phys. Rev. Lett. **69**, 1540 (1992).
[54] Y. Inamura, M. Arai, N. Kitamura, S. M. Bennington, and A. C. Hannon, Physica B **241-243**, 903 (1998).
[55] U. Buchenau, N. Nücker, and A. J. Dianoux, Phys. Rev. Lett. **56**, 539 (1986).
[56] J. Mattsson, A. Matic, G. Monaco, D. Engberg, and L. Börjesson, J. Phys.: Condens. Matter **15**, S1259 (2003).
[57] G. Monaco, C. Masciovecchio, G. Ruocco, and F. Sette, Phys. Rev. Lett. **80**, 2161 (1998).
[58] D. Fioretto, U. Buchenau, L. Comez, A. Sokolov, C. Masciovecchio, A. Mermet, G. Ruocco, F. Sette, L. Willner, B. Frick *et al.*, Phys. Rev. E **59**, 4470 (1999).
[59] V. N. Novikov and A. P. Sokolov, Nature (London) **431**, 961 (2004).
[60] V. N. Novikov, Y. Ding, and A. P. Sokolov, Phys. Rev. E **71**, 061501 (2005).
[61] M. A. Ramos, S. Vieira, F. J. Bermejo, J. Dawidowski, H. E. Fischer, H. Schober, M. A. González, C. K. Loong, and D. L. Price, Phys. Rev. Lett. **78**, 82 (1997).
[62] A. Matic, C. Masciovecchio, D. Engberg, G. Monaco, L. Börjesson, S. C. Santucci, and R. Verbeni, Phys. Rev. Lett. **93**, 145502 (2004).